1994ApJ...426..704L

THE ASTROPHYSICAL JOURNAL, 426:704–715, 1994 May 10
© 1994. The American Astronomical Society. All rights reserved. Printed in U.S.A.

OBSERVATIONS OF THE BRIGHT NOVALIKE VARIABLE IX VELORUM WITH THE HOPKINS ULTRAVIOLET TELESCOPE

KNOX S. LONG
Space Telescope Science Institute, 3700 San Martin Drive, Baltimore, MD 21218
long@stsci.edu

RICHARD A. WADE
Department of Astronomy & Astrophysics, Pennsylvania State University, University Park, PA 16802
wade@astro.psu.edu

WILLIAM P. BLAIR AND ARTHUR F. DAVIDSEN
Department of Physics & Astronomy, The Johns Hopkins University, Baltimore, MD 21218
wpb@pha.jhu.edu, afd@pha.jhu.edu

AND

IVAN HUBENY
NASA Goddard Space Flight Center, Greenbelt, MD 20771
hubeny@stars.gsfc.nasa.gov
Received 1993 September 30; accepted 1993 November 11

ABSTRACT

The Hopkins Ultraviolet Telescope, an experiment flown on the Space Shuttle as part of the *Astro-1* mission, was used to obtain a spectrum of the novalike variable IX Vel (= CPD −48°1577) in the wavelength range 830–1860 Å. The observation revealed a rich absorption-line and continuum spectrum that peaks near 1050 Å at a flux of 1.6×10^{-11} ergs cm^{-2} s^{-1} Å^{-1}. In the sub–Lyman-α region, some of the more prominent absorption lines are S VI λλ933, 945, C III λ977, Lyman-β, O VI λλ1032, 1038, P V λλ1118, 1128, and C III λ1176. No emission was detected below the Lyman limit. The overall continuum shape of IX Vel in the FUV can be approximated using models of an optically thick accretion disk in which the integrated spectrum has been constructed by summing model stellar atmospheres or proper disk model spectra. However, if the distance to IX Vel is ∼95 pc, standard disk models without reddening cannot simultaneously reproduce the color and flux in the UV. While interstellar reddening can reconcile this difference, the amount of reddening appears inconsistent with the absence of a 2200 Å bump in the spectrum and the very low H I column density measured along the line of sight. Improved fits to the data can be obtained by modifying the accretion disk structure within three white dwarf radii. None of the models reproduces the profiles of the Li- and Na-like ions, which are observed as strong but relatively narrow absorption lines, and which are almost surely due to a wind above the disk.

Subject headings: binaries: close — novae, cataclysmic variables — stars: individual (IX Velorum) — ultraviolet: stars

1. INTRODUCTION

In nonmagnetic cataclysmic variables (CVs), mass flows from a relatively normal, cool, main-sequence star and forms an accretion disk around a white dwarf (WD). In dwarf novae, changes in the state of the accretion disk (often parameterized in terms of changes in the mass accretion rate in the inner portion of the disk) are responsible for the outbursts which are observed at optical and UV wavelengths. Novalike variables are CVs that appear to be stuck in the high state, presumably because the time-averaged accretion rate is higher in these systems than in dwarf novae. They are important not only because they constitute one of the major subclasses of CVs, but specifically because their accretion disks are more likely to be in a steady state than those in dwarf novae in outburst. Therefore the disks of novalike variables are presumably more straightforward to compare with detailed models of accretion disks.

IX Vel (= CPD −48°1577), which has a period of 4.65 hr, is the brightest CV ($m_v = 9.7$) and the only novalike variable in which the secondary has been observed (Haug 1988). From an orbital study of emission lines from the secondary star, Beuermann & Thomas (1990, hereafter BT) infer an inclination for the system of 60° ± 5° and masses for the WD and normal companion of ∼0.8 and 0.5 $M_\odot$, respectively. From the IR brightness of the secondary, they derive a distance to IX Vel of 95 ± 12 pc, which together with the visual magnitude for (the disk in) IX Vel suggests a mass accretion rate of 5×10^{17} g s^{-1}.

As observed with *IUE*, the ultraviolet spectrum of IX Vel resembles that of low-inclination dwarf novae in outburst, rising steeply toward the shortest wavelengths (Sion 1985). N V λ1240, Si III + O I λ1300, Si IV λλ1394, 1403, C IV λλ1548, 1551, and He II λ1640 are observed in absorption. As is common in other noneclipsing systems, the C IV doublet has a strong P Cygni profile, and other resonance transitions—S IV and N V—have absorption wings which extend blueward by 2000–3000 km s^{-1} (Sion 1985; Mauche 1991). These features are presumed to arise from an extended wind in the system seen against the continuum light of the accretion disk (see, e.g., Drew 1987; Mauche & Raymond 1987).

IX Vel is one of about six CVs that have been observed with the *Voyager* Ultraviolet Spectrometers in the wavelength range between Lyman-α and the Lyman limit (Polidan, Mauche, & Wade 1990). The low-resolution (18 Å) *Voyager* spectrum of IX Vel shows f_λ declining moderately from 1150 Å

© American Astronomical Society • Provided by the NASA Astrophysics Data System

1994ApJ...426..704L

toward shorter wavelengths. A single broad absorption feature is observed, which is identified with a blend of O VI and Lyman-β.

Here we describe a higher resolution 830–1860 Å spectrum of IX Vel obtained with the Hopkins Ultraviolet Telescope on the *Astro-1* Space Shuttle mission. Four other CVs were observed with this telescope, including an eclipsing novalike variable—UX UMa (Long 1993)—and a dwarf nova in outburst—Z Cam (Long et al. 1991).

2. OBSERVATIONS

The Hopkins Ultraviolet Telescope (HUT) consists of a 0.9 m Ir-coated f/2 primary mirror which focuses light onto a Rowland spectrograph located at the prime focus (Davidsen et al. 1992). Photons enter one of several selectable apertures and are diffracted by an Os-coated concave grating onto a microchannel plate-intensified, photodiode array detector. The spectrograph and detector system have an intrinsic resolution of $\sim$3 Å and cover the wavelenth range 830–1860 Å in first order. The resolution can be degraded somewhat by jitter of the Space Shuttle's Instrument Pointing System that was used to position the telescope on the sky. The payload and mission specialists aboard the Shuttle used a slit-jaw camera to position the telescope.

The observation of IX Vel took place during orbital day on 1990 December 10. Acquisition was straightforward; IX Vel and two pre-identified guide stars were visible with the HUT slit-jaw camera. Approximately 300 s of data were obtained beginning at GMT 1:30:10, corresponding to orbital phase 0.27 ± 0.01, that is, near quadrature, according to the ephemeris derived by BT. Prior to the on-source portion of the observation, during the time when the playload specialists were acquiring the target, about 28 s of airglow data were also obtained.

Unfortunately, to our knowledge no contemporaneous ground-based observations are available to help establish the state of the system. The V magnitude of the system varies, on timescales of a day or longer, between rough limits of 9.4 and 9.9 (Wargau et al. 1983; Eggen & Niemela 1984; Garrison et al. 1984). The larger variations seem to occur on longer timescales. Observations on timescales of minutes have not shown variations larger than $\sim$10% (Williams & Hiltner 1984; Warner, O'Donoghue, & Allen 1985).

IX Vel is a very bright source in the HUT spectrograph. An average count rate of 3300 s^{-1} was observed. The count rate varied considerably throughout the observation from a peak value of 4150 s^{-1} to a minimum value of 1750 s^{-1}. An inspection of the images obtained with the HUT slit-jaw camera prior to and during the HUT observation suggests that IX Vel was not well centered in the 18″ diameter aperture that was used for the observation. The fact that the shape of the spectrum remains the same over the entire HUT wavelength range supports this hypothesis; there is no evidence for intrinsic variations in IX Vel during this brief observation.

Information about pointing jitter during observations with HUT can be obtained from the positions of guide stars in the HUT camera and from the image motion control system (used to provide error signals to the other experiments on *Astro*). The rms pointing error for the observation was $\sim$2″ (in each axis) for the IX Vel observation. An offset of the position of a point source by 3″ in the direction of the dispersion axis corresponds to a wavelength shift of 1 Å. Taking the intrinsic resolution of HUT to be 3 (3.5) Å, the effect of jitter is to degrade the spectral resolution only slightly to 3.4 (3.8) Å.

The position of IX Vel in the slit affects the wavelength calibration of the spectra obtained. The TV images indicate that the IX Vel spectrum was redshifted relative to the nominal on-axis calibration. Assuming that the flux from IX Vel was constant throughout the observation, it is possible to find the position of IX Vel in the HUT aperture by correlating the pointing errors with the counting rate. For IX Vel, this analysis indicates that the spectrum was redshifted from its true value by $\sim$1.3 Å. Thus in the figures, a feature at apparent wavelength λ corresponds to a corrected wavelength of $\lambda - 1.3$ Å (except lines from airglow, which filled the aperture).

Inspection of the raw spectrum of IX Vel shows no evidence for emission below the Lyman limit. The count rate of 0.0133 s^{-1} $pixel^{-1}$ observed between 850 and 890 Å is that expected due to grating scattered light in the HUT detector. (The count rate also includes a small contribution of about 0.0005 s^{-1} $pixel^{-1}$ due to dark counts in the HUT detector.) In this case, reduction of the HUT spectrum is straightforward. Corrections are made for scattered light (using the sub-Lyman limit rate), for doubly counted events (which arise due to persistence in the phosphor in the HUT detector), and for second-order photons (which affect the first-order spectrum beyond 1824 Å), and then the spectrum is flux-calibrated using the response function described by Davidsen et al. (1992). Because IX Vel is so bright there is little effect of airglow on the on-source data, except at the positions of O I $\lambda\lambda$989–991, N I λ1200, Lyman-α, and O I $\lambda\lambda$1304, 1356. Nevertheless, we did attempt to use the flux-calibrated airglow spectrum obtained just prior to the observation to remove airglow from the source spectrum. Airglow emission varies even on timescales of 300 s, and therefore it is not surprising that some residual emission remains at O I $\lambda\lambda$1304, 1356. Finally, we have multiplied the resultant spectrum by 1.25 (= 4150/3300) to correct for the fact that IX Vel was not completely in the slit at all times.

The flux-calibrated spectrum is shown in Figure 1. It peaks at 1050 Å at 1.6×10^{-11} ergs cm^{-2} s^{-1} $Å^{-1}$. The flux declines shortward of 1050 Å, but emission is clearly seen to the Lyman limit. The overall flux level that we observed is in rough agreement with the values obtained with *IUE* (Sion 1985; Haug 1987; La Dous 1990) and with *Voyager* data near 1000 Å (Polidan et al. 1990), although the *Voyager* flux continues to rise further to the red. (IX Vel appears to show long-term variations no larger than a factor of 1.5 as observed with *IUE*; see La Dous 1990. Note that Verbunt 1987 tabulates fluxes lower by $\sim$50% than given by Haug 1987 or La Dous 1990, using the same pair of *IUE* spectra.)

A continuum-normalized version of the spectrum is shown in Figure 2. The continuum spectrum we used to normalize the spectrum was obtained by fitting the flux-calibrated spectrum to a tenth-order spline function. Regions with absorption lines were preferentially excluded from the continuum fit. After dividing the flux-calibrated spectrum by the continuum, we fit the normalized spectrum to a series of Gaussians in order to obtain estimates of the equivalent widths and full widths at half-maxima (FWHM) of the absorption features. The results of these fits as well as the proposed line identifications are presented in Table 1. The overall fit to the renormalized spectrum is shown in Figure 2. Above Lyman-α, the $2s$–$2p$ ground-state transitions of Li-like C IV $\lambda\lambda$1548, 1551 and N V $\lambda\lambda$1239, 1243 are observed; the HUT spectrum shows the extension of this isoelectronic sequence below Lyman-α, where the same transition is observed in O VI $\lambda\lambda$1032, 1038. Above Lyman-α, the $3s$–$3p$ ground-state transition in Na-like Si IV $\lambda\lambda$1394, 1403 is observed; below Lyman-α, this sequence is now extended to

© American Astronomical Society • Provided by the NASA Astrophysics Data System

1994ApJ...426..704L

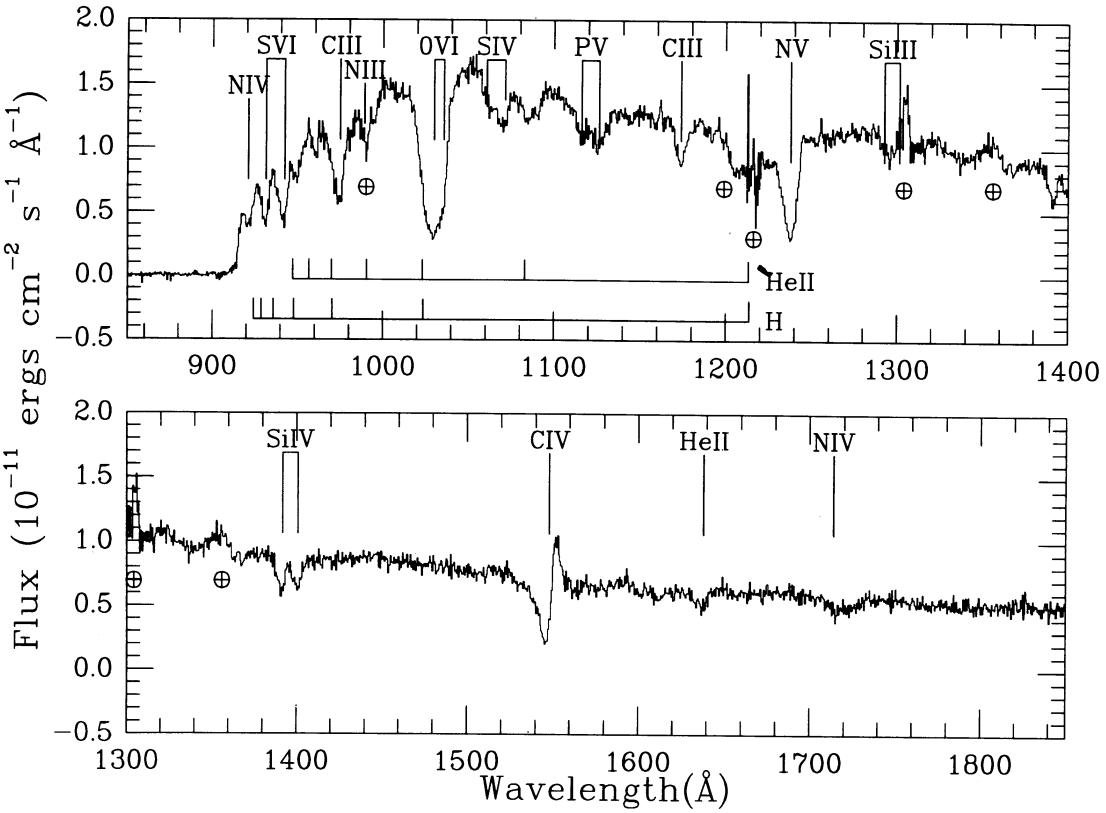

FIG. 1.—Flux-calibrated 830–1860 Å spectrum of IX Vel as observed with HUT. Prominent absorption lines in the spectrum are labeled. (Note: The positions of the labels for the absorption lines have been blueshifted by 2 Å.)

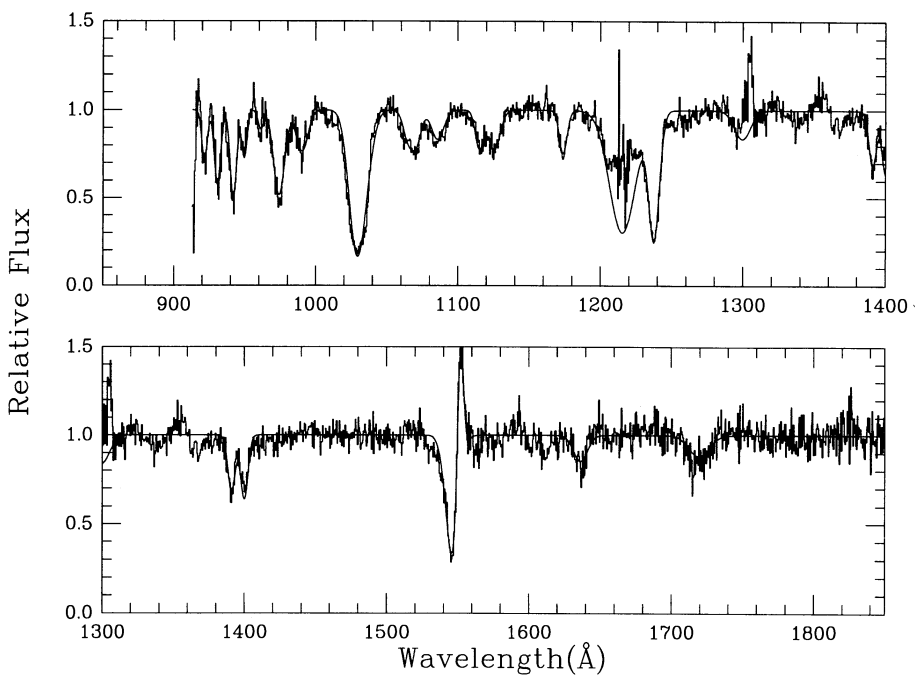

FIG. 2.—Line spectrum of IX Vel after renormalizing the raw spectrum. The continuum spectrum used for this renormalization was a tenth-order spline function. Regions with absorption were preferentially excluded from the fit. The renormalized spectrum was fitted to a series of Gaussian absorption (and emission) lines as indicated by the solid curve. The results, along with suggested line identifications, are summarized in Table 1.

© American Astronomical Society • Provided by the NASA Astrophysics Data System

1994ApJ...426..704L

TABLE 1

STRONG LINES: IX Vel

Ion	λ_{lab} (Å)	λ_{obs}[a] (Å)	EW (Å)	FWHM (Å)
N IV	923	920.28 ± 0.20	−1.37 ± 0.11	4.61 ± 0.49
S VI[b]	933	929.46 ± 0.09	−2.39 ± 0.11	5.37 ± 0.18
S VI[b]	945	940.63 ± 0.09	−2.87 ± 0.10	5.43 ± 0.18
H I	950	948.44 ± 0.27	−1.30 ± 0.11	4.57 ± 0.39
		960.08 ± 0.67	−0.53 ± 0.12	4.64 ± 0.88
C III	977	972.87 ± 0.17	−4.70 ± 0.13	9.13 ± 0.31
N III	991	988.99 ± 0.41	−2.42 ± 0.16	9.71 ± 0.70
H I[c]	1026	1024.90 ± 0.10	−4.29 ± 0.11	11.84 ± 0.18
O VI[c]	1032	1029.10 ± 0.10	−6.09 ± 0.10	11.89 ± 0.18
O VI[c]	1038	1034.80 ± 0.10	−2.63 ± 0.12	11.96 ± 0.18
S IV[b]	1063	1063.60 ± 0.46	−1.36 ± 0.15	7.99 ± 0.45
S IV[b]	1073	1069.60 ± 0.46	−1.53 ± 0.15	8.03 ± 0.45
He II	1085	1084.50 ± 0.62	−1.80 ± 0.17	10.18 ± 0.83
		1113.80 ± 0.43	−1.51 ± 0.14	6.73 ± 0.55
P V[b]	1119	1118.30 ± 0.43	−0.09 ± 0.17	9.65 ± 0.70
P V[b]	1128	1124.30 ± 0.43	−2.29 ± 0.16	9.70 ± 0.70
C III	1175–1176	1172.70 ± 0.32	−1.68 ± 0.13	6.46 ± 0.49
H I	1215	1214.40 ± 0.26	−16.14 ± 0.66	21.69 ± 0.73
N V	1239, 1242	1236.60 ± 0.10	−6.64 ± 0.10	8.77 ± 0.15
S III[d]	1300	1298.30 ± 1.09	−2.30 ± 0.48	13.25 ± 3.18
Si IV[b]	1394	1389.80 ± 0.19	−2.09 ± 0.12	6.17 ± 0.27
Si IV[b]	1403	1398.90 ± 0.19	−2.39 ± 0.13	6.21 ± 0.27
C IV[e]	1548, 1551	1545.20 ± 0.14	−8.26 ± 0.14	11.35 ± 0.22
C IV[e]	1548, 1551	1550.80 ± 0.09	4.46 ± 0.15	4.95 ± 0.16
He II	1640	1635.10 ± 0.62	−176 ± 0.18	11.36 ± 0.33
N IV	1718	1718.40 ± 0.90	−2.09 ± 0.22	16.32 ± 1.29

[a] Observed wavelengths have been corrected by 1.3 Å to account for the position of IX Vel in the aperture.

[b] Fit as doublet. The line strengths were allowed to vary independently, but the relative position of the lines was fixed and the FWHM were constrained to be the same (in velocity space).

[c] Hβ and O VI λλ1032, 1038 were fitted as if they were a triplet in which the relative wavelengths of the lines were fixed and the FWHM were identical, but in which the strength of each component was allowed to vary.

[d] Only the short wavelenth portion Si III λλ1295–1303 was fitted due to residual contamination from O I λ1304.

[e] C IV λλ1548, 1551 was fitted in terms of two Gaussians corresponding to the absorption and emission portions of the profile.

include P V λλ1118, 1128 and S VI λλ933, 945. Additional transitions in the newly observed spectral region below Lyman-α include N IV λ923, C III λ977, and C III λ1176. The first three Lyman lines of H are blended; the higher lines do not appear strongly, perhaps because of strong velocity smearing (see § 3). The 2–3 λ1640 transition and likely the 2–5 λ1085 transition of He II are present but not strong in comparison with the ground-state transitions noted above. Most of the lines are blueshifted by 2–3 Å using standard on-axis wavelength calibration, or 3–4 Å when the position of IX Vel in the aperture is taken into account.

The rich absorption-line spectrum shortward of Lyman-α resembles that of Z Cam, which was observed in outburst with HUT (Long et al. 1991). This similarity extends to the continuum shape as well, as is shown in Figure 3. Inspection shows several differences apart from those due to lower S/N ratio and higher airglow contamination in the IX Vel spectrum. First, the narrow absorption features shortward of 950 Å are stronger and appear at shorter wavelengths in IX Vel. Second, the continuum in the 950–970 Å region is relatively brighter in Z Cam compared with IX Vel. Third, although a rapidly changing airglow emission from O I λλ989–991 might partially account for the difference, N III λ991 appears to be weaker in IX Vel. Fourth, the He II λ1640 line in Z Cam clearly shows a P Cygni–like emission component, while this line in IX Vel is all or mainly in absorption. Fifth, Z Cam shows strong absorption at 1371 Å due to O V while IX Vel does not. Finally, the N IV λ1718 line in the same isoelectronic sequence as O V also appears stronger in Z Cam, although in both stars there is likely an additional contributor, possibly Si IV λλ1722, 1725.

3. ANALYSIS

We would like to be able to use the HUT spectrum of IX Vel to better understand the temperature and structure of the accretion disk, and to determine whether there is evidence for additional components to the emission, such as the WD or a disk-star boundary layer. The ultraviolet emission arises predominantly from the accretion disk, but the disk spectrum is viewed through a wind. We briefly discuss the line spectrum first, in order to clarify what parts of the IX Vel spectrum a disk model per se should explain.

3.1. *Absorption Lines*

The fact that C IV λλ1548, 1551 has a classic P Cygni profile with a red emission wing shows that there was a wind present in IX Vel at the time of the HUT observation. Although none of the other lines has an emission component, it is quite likely that many of them arise in the wind as well, especially since the centroids of these lines are blueshifted by 3–4 Å. One expects emission wings only if the line-scattering region (for a particular ion) has a larger solid angle than the underlying continuum emitting region. Drew (1987) and Mauche & Raymond (1987) have shown that this is often not the case for plausible CV disk and wind geometries. They also noted that blueshifted centroids should be more common than classic P Cygni features due to partial filling of the red wing of the absorption profile by emission. Moreover, HUT observations of the novalike variable UX UMa during an eclipse of the disk by the companion show *in emission* nearly all the strong lines seen in absorption in IX Vel, indicating the presence of scattering or emitting ions far away from the inner disk in that system (Long 1993).

Mauche (1991) used high-resolution spectra obtained with *IUE* to determine the centroid of Si IV λλ1394, 1403 as a function of orbital phase in IX Vel. He found that the velocity centroid of Si IV λλ1394, 1403 varies sinusoidally approximately as $v_{\rm Si\,IV} = -351 + 201 \times \sin [2\pi(\phi + 0.39)]$ km s^{-1}, which differs from the radial velocity solution for the WD and accretion disk $v_{\rm wd} = 48 + 138 \times \sin [2\pi(\phi + 0.5)]$ km s^{-1}. At the phase of the HUT observation, Mauche's data suggest $v_{\rm Si\,IV}$ of -520 km s^{-1} or a blueshift of about 2.4 Å. The blueshift we observe, 3.9 Å, when the offset of IX Vel in the aperture is taken into account, is somewhat larger than this, but is certainly consistent with the hypothesis that Si IV λλ1394, 1403 is arising in the wind.

As will be discussed in the next sections, there is some correspondence between features in the disk models and the observed spectrum for the lower ionization lines, particularly in the region between 1050 and 1200 Å. In addition, Lyman-γ + C III λ977, Lyman-β, Lyman-α, and Si III λλ1295–1303 are clearly evident in our models (though in the IX Vel spectrum Lyman-α, Lyman-β, and Si III λλ1295–1303 unfortunately are contaminated by airglow and, in the case of Lyman-β, by O VI λλ1032, 1038).

Generally speaking, however, the models lead us to expect that the strong lines seen in the observed spectrum arise from some other location than the disk itself. Doppler smearing is part of the reason it is difficult to reproduce the relatively

© American Astronomical Society • Provided by the NASA Astrophysics Data System

1994ApJ...426..704L

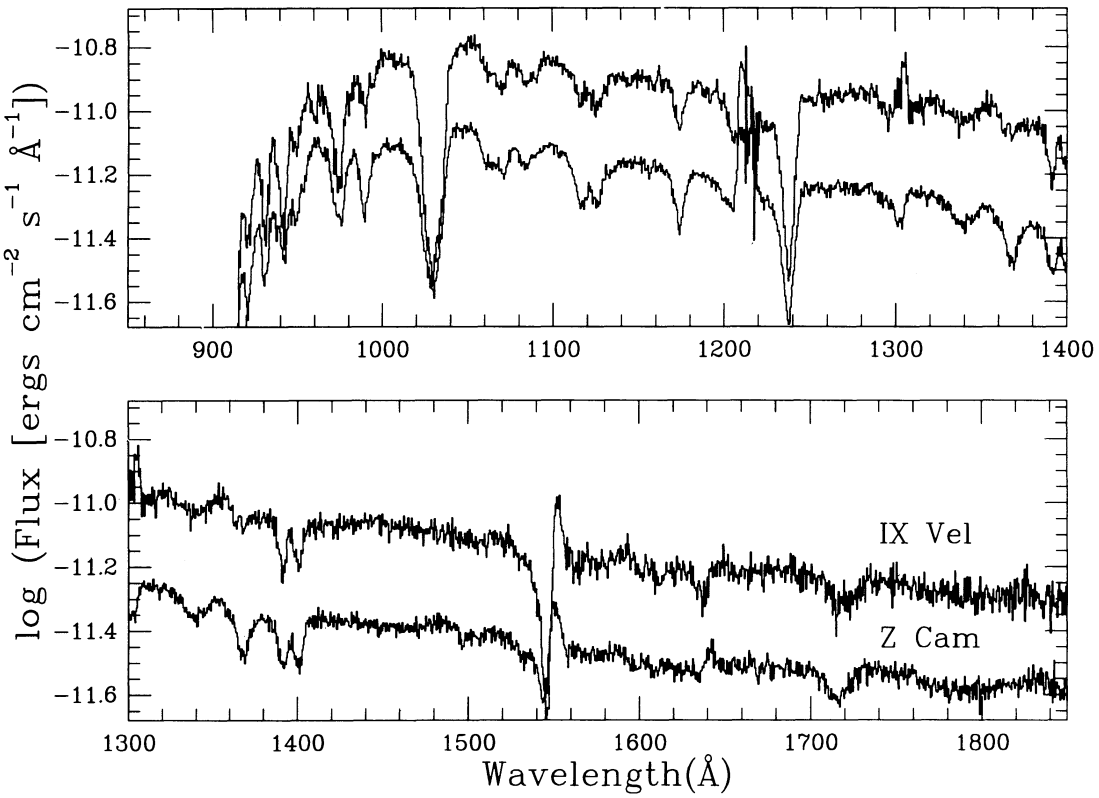

FIG. 3.—Comparison between the HUT spectra of IX Vel and Z Cam. The Z Cam spectrum has been rescaled to fit on the plot and blueshifted 4 Å so that the lines common to it and IX Vel are aligned. Except for an overall normalization, the spectra of IX Vel, a novalike variable, and Z Cam, a dwarf nova observed in outburst, are very similar. The differences between the two are described in the text.

narrow absorption lines we see in IX Vel using disk models. The continuum at short wavelengths is formed mainly in the inner disk. The projected circular orbital speed two WD radii from the center of an 0.8 $M_\odot$ WD viewed at 60° inclination is $\sim$3400 km s^{-1}, corresponding to roughly $\pm$11 Å at 1000 Å. Disk line profiles concentrate much of the equivalent width near the extreme velocities, rather than near the center of the line as for a rotating star. Furthermore, the high-ionization lines—S VI $\lambda\lambda$933, 945, O VI $\lambda\lambda$1032, 1038, P V $\lambda\lambda$1118, 1128, N V $\lambda\lambda$1239, 1243, Si IV $\lambda\lambda$1394, 1403, and C IV $\lambda\lambda$1548, 1551—are difficult to produce because the appropriate ions do not exist in sufficient numbers in the model photospheres of the hottest, innermost portion of the disk to overcome the diluting effect of the continuum from farther out in the disk. In the models discussed below roughly two-thirds of the disk continuum at 1000 Å is produced in regions where $T_{\rm eff}$ is below 45,000 K.

There are as yet no "unified" models of disk + wind spectra, nor even full wind models for CVs, although detailed models of individual lines have been produced (see, e.g., Hoare & Drew 1993; Shlosman & Vitello 1993; Vitello & Shlosman 1993). In particular it is not possible to predict with assurance the shapes and relative strengths of the various wind lines, since the radial ionization structure and the angular density profile of the wind are still in dispute (e.g., Mauche & Raymond 1987). We therefore confine our attention in the remainder of this paper to accounting for the continuum (and weak disk lines) against which the strong wind lines appear.

3.2. *Modeling the Disk Continuum*

We will consider only steady state accretion disks and simple, illustrative modifications of them. Our goal is the limited one of exploring whether the HUT spectrum can be described in terms of a steady state disk, or whether modifications are clearly demanded by the data.

For a steady state accretion disk around a nonrotating star, the effective temperature at radius r of the disk is given by

$$T_{\rm eff} = T_* x^{-3/4}(1 - x^{-1/2})^{1/4}\ {\rm K}\ , \qquad (1)$$

where

$$T_* = 107{,}000\left[\left(\frac{M_{\rm wd}}{1\ M_\odot}\right)\left(\frac{\dot m}{10^{17}\ {\rm g\ s^{-1}}}\right)\left(\frac{R_{\rm wd}}{6\times 10^8\ {\rm cm}}\right)^{-3}\right]^{1/4}, \qquad (2)$$

and

$$x = \frac{r}{R_{\rm wd}} \qquad (3)$$

(see, e.g., Polidan et al. 1990). The WD mass and orbital inclination for IX Vel were estimated by BT. They are 0.8 (+0.16, −0.11) $M_\odot$ and 60° $\pm$ 5°, respectively. To limit the number of adjustable parameters in the model, we adopt fixed values of 0.8 $M_\odot$ and 60°. We adopt a radius of 6.985 × 10^8 cm for the WD. This leaves $T_{\rm eff}(r)$ to be determined solely by the accretion rate. BT estimate the distance of IX Vel to be 95 $\pm$ 12 pc, and

© American Astronomical Society • Provided by the NASA Astrophysics Data System

1994ApJ...426..704L

for their own assembly of observations (*IUE* through infrared) derive a steady state accretion rate of 5×10^{17} g s^{-1}.

3.2.1. "*Stellar*" *and* "*True*" *Disk Models*

In this paper we make use primarily of disk spectra constructed on the assumption that each annulus of the disk radiates as a stellar atmosphere with the same temperature and gravity as a steady state disk. This assumption is very unlikely to be correct in detail, since the conditions in accretion disks differ substantially from those in stars (see, e.g., Kriz & Hubeny 1986; Shaviv & Wehrse 1991). The differences include the facts that (1) energy is (presumably) generated throughout the atmosphere of disks, but not stars, (2) the gravitational acceleration varies with height in disks but not (substantially) in stars, and (3) disks may not be everywhere optically thick at the midplane. Therefore, before using models based on stellar atmospheres, we discuss calculations of a representative model in which the disk spectrum is calculated self-consistently. We conclude that, at the high accretion rates likely to obtain in the disk of IX Vel, the effect of these differences on the *far-UV spectrum* are minimal due to the high optical depth, which reduces (1) and (3) in importance, and that we are not compromising our results by using computationally simpler models based on model stellar atmospheres.

Disk spectra constructed from stellar model atmosphere spectra (hereafter called simply "stellar" disk spectra) are constructed by summing area-weighted contributions from spectra which are labeled by effective temperature and gravity (see, e.g., Wade 1984, 1988). To establish this gravity, we have used the prescription given by Herter et al. (1978) derived from the assumption that the half-thickness of the accretion disk is

$$z(r) = \frac{v_s}{v_\phi} r \tag{4}$$

where v_s/v_ϕ is the ratio of the sound speed to the Keplerian velocity at radius r.

The HUT spectra have higher resolution than the Kurucz models used in the past for most comparisons with *IUE* or *Voyager* data. Therefore, we have constructed a new grid of stellar spectra ($5000 < T < 115{,}000$ K, $3 < \log g < 8$; the exact gravity range depends on T). At 10,000 K and above, we used the program TLUSTY (Hubeny 1988) to calculate the temperature and density structure of the atmosphere. For these structure calculations, opacities were based on H, He, C, N, and O. Below 10,000 K, we used model atmospheres calculated by Kurucz (1993). In all cases we used the program SYNSPEC (Hubeny 1994b) to calculate the detailed spectrum assuming cosmic abundances and using the Kurucz (1990) line list, which contains $\sim$120,000 lines in the HUT wavelength range. All calculations assumed LTE. The spectra were initially calculated on a wavelength grid with a maximum separation of 0.015 Å and then convolved to the HUT resolution of 3 Å (FWHM) and sampling interval of 0.513 Å.

We constructed the model "stellar" accretion disk spectra by summing appropriately weighted and Doppler-broadened stellar spectra in each radial zone of the disk. We used the WD mass and radius and the orbital inclination specified above. We adopted an outer disk radius of 4×10^{10} cm and various accretion rates ranging from 5×10^{14} to 2×10^{18} g s^{-1}.

The "stellar" disk models use angle-averaged spectra, H_λ, appropriate for stars. We also used SYNSPEC to calculate specific intensities, $I_\lambda(\mu)$, for a somewhat smaller set of the stellar models. Disks constructed for various inclinations i showed an overall diminution in the flux seen by a distant observer as i increased, but the shape of the spectrum did not change significantly, at least until the inclination angle exceeded 75° ($\mu = \cos i = 0.25$).

We have recently begun a program to calculate accretion disk spectra using the method described by Kriz & Hubeny (1986) and Hubeny (1990) to calculate self-consistently the structure of the disk with the radiation field. Here we call these models "true" disk spectra. We retain the assumption that the emergent radiation from the disk can be constructed from a set of concentric rings, each radiating independently. In other words, we neglect radial energy transport or any interaction with other zones of the disk, for example, by irradiation. We also assume that the total energy (labeled by $T_{\rm eff}$) that must be radiated by each ring is given by equations (1)–(3). However, we calculate the vertical structure of each ring by simultaneously solving the *disk* equations of hydrostatic equilibrium, the radiative transfer equation, and the energy balance. The difference from the stellar case arises because the hydrostatic equation and the boundary conditions of the radiative transfer equation, as well as the energy dissipation in the disk, are different for stars and disks. For simplicity, we assume local thermal equilibrium (LTE), so the statistical equilibrium equations are not solved. The computer code TLUSDISK implements this prescription for the vertical structure. The spectrum of each ring is computed as before, using SYNSPEC and the Kurucz (1990) line list. The integrated disk spectrum is assembled using the code DISKSYN, optionally taking into account occultation of part of the disk by the central star.

We assume that the viscosity in the "true" disk models is given by the Reynolds number prescription (Lynden-Bell & Pringle 1974; Kriz & Hubeny 1986), viz.,

$$\bar{\nu} = (GM_{\rm wd} R_{\rm wd})^{1/2}/Re \tag{5}$$

where $\bar{\nu}$ is the vertically averaged kinematic viscosity and Re is the Reynolds number, taken as a free parameter. We have adopted the value $Re = 5000$ (Lynden-Bell & Pringle 1974; Kriz & Hubeny 1986) for all present models. Further, we assume the local viscosity can be parameterized in Lagrangian mass coordinates in terms of a power-law relation

$$\nu = \bar{\nu}(\zeta + 1)(m/M)^\zeta , \tag{6}$$

where m is the Lagrangian mass coordinate defined by

$$m = \int_z^\infty \rho \, dz , \tag{7}$$

$M = \Sigma/2$ is the Lagrangian mass at the central plane, and ζ is another free parameter (Kriz & Hubeny 1986). If ζ is large then the viscosity decreases rapidly as a function of z while for $\zeta = 0$ the viscosity is constant with height, which may lead to a large (sometimes catastrophic) increase of the local temperature at the surface (see also Shaviv & Wehrse 1986); $\zeta = \frac{2}{3}$ is adopted for most models discussed below.

Figure 4 shows a comparison of a "stellar" disk spectrum and a "true" disk spectrum, computed for the same accretion rate, WD mass and radius, inclination, and distance. (Note that different codes were used by different authors to carry out the summation of annuli and the Doppler broadening and regridding of the spectra in the two cases. Different grids of $T_{\rm eff}$ were also used.) The shape of the continuum is closely similar in the two model spectra. The offset of $\sim$15% in overall flux level is due to the difference between H_λ (used in the "stellar" model) and $I_\lambda(\mu = 0.50)$ (used in the "true" model). This difference is

© American Astronomical Society • Provided by the NASA Astrophysics Data System

1994ApJ...426..704L

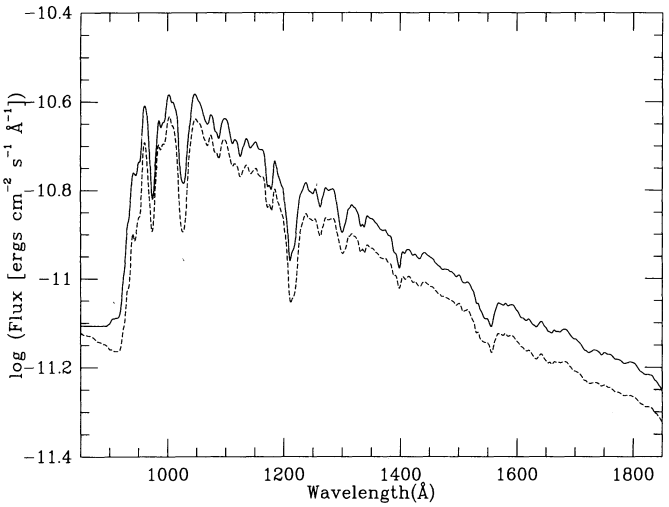

FIG. 4.—Comparison between a "stellar" disk spectrum (*solid curve*) and a "true" disk spectrum (*dashed curve*). Both model spectra were calculated for $\dot{m} = 3 \times 10^{17}$ g s^{-1}, $M_{wd} = 0.8\ M_\odot$, and $r_{wd} = 6.985 \times 10^8$ cm.

due to limb darkening. With zero limb darkening $H_\lambda = I_\lambda(\mu = 0.50)$.

It is interesting to compare the gravitational acceleration in the photosphere of each annulus in the "true" disk with that of the "stellar" model. We define "equivalent gravity" here to mean the tidal gravity $g = GM_{wd}\, z/r^3$ measured at distance z from the midplane where the vertical Rosseland optical depth is unity. For the "true" model shown in Figure 4, the equivalent gravity runs from $\log g = 6.7$ near $r = R_{wd}$ to $\log g = 4.4$ at the radius where T_{eff} has fallen to 11,000 K, $r = 26R_{wd}$. Over the same range, the "stellar" disk gravity computed using the Herter et al. (1978) formula runs from $\log g = 6.0$ to 3.5. (A comparison of gravities in this way is essentially a comparison of the height of the photosphere from the disk midplane. Of more interest to the question of spectrum formation would be a comparison of the gas pressure at optical depths near unity, which we have not undertaken.)

We conclude that, *for our present exploration of the far-UV spectrum of IX Vel*, little is gained by preferring "true" disks over "stellar" disks. This is because of the large optical depth (measured normal to the disk plane) of the IX Vel disk, at least in the parts that contribute to the far-UV spectrum. Large optical depth hides a multitude of inconsistencies. Since the "true" disks are computationally more expensive, we will for the remainder of this paper use "stellar" disk spectra as described above. We stress that we are ignoring possibly interesting effects such as irradiation of a disk zone from the central star, its boundary layer, or elsewhere in the disk; NLTE effects; and backwarming from a "wind albedo." These sorts of "complications" will eventually require "true" disk models, as will attempts to model the Balmer jump (see, e.g., Hubeny 1994a) and other parts of the spectrum where optical depth effects are critical.

We did use a "true" disk annulus to investigate the effect of changes in ζ. Varying ζ over a reasonable range does not appear to affect the far-UV spectrum significantly for an annulus at 25,000 K computed using the model parameters described above. Although with lower values of ζ the gas temperature is a few hundred K larger at very low optical depths, by the time the optical depth reaches unity the temperature is almost identical for $\zeta = 0$, one-third, or two-thirds. The reason is again that the midplane optical depth τ of this annulus is of order 300, so that in any of the cases tried most of the viscous dissipation occurs below the spectrum-forming layers.

3.2.2. *"Stellar" Disks Compared with IX Vel*

A comparison of the IX Vel spectrum to three models having mass accretion rates of 6×10^{15}, 6×10^{16}, and 6×10^{17} g s^{-1} is shown in Figure 5. All of the models have been scaled to match the HUT spectrum at 1425 Å, and the corresponding distances are noted in the caption. It is assumed that there is no reddening; an interstellar contribution to the model Lyman-α profiles has been added using a neutral H column density of 2×10^{19} cm^{-2}, as estimated by Mauche, Raymond, & Córdova (1988). (The primary effect of including neutral H absorption is to affect small regions near Lyman-α and the Lyman limit.) In the region longward of Lyman-α where there are relatively few strong absorption lines, all of the three models approximate the observed continuum shape well. (Note: As the accretion rate is lowered, the color temperature of the model spectrum drops and the width and depth of the Lyman-α line increase. Models with $\dot{m} < 2 \times 10^{16}$ g s^{-1} fail both in the restricted range from 1200–1850 Å and, more dramatically, in matching the overall flux distribution.)

An optimum value of $\dot{m}$ was obtained by fitting the data using a χ^2 minimization routine. For these fits, the two free parameters were the normalization—effectively the distance to the source—and the mass accretion rate $\dot{m}$. All of the data between 912 and 1860 Å were included in the fits, except for the strong airglow lines—N I λ1200, Lyman-α, and O I λλ1304, 1356—and the 2*s*–2*p* or 3*s*–3*p* resonance lines of S V, O VI, N V, and Si IV. A model with $\dot{m} = 6 \times 10^{16}$ g s^{-1} best approximates the overall continuum shape, and it matches especially closely the slope in the region of the spectrum longward of Lyman-α. (Even so, the rms error between the model and the spectrum is ~10%.) Fits restricted to the long-wavelength portion of the spectrum yield the same $\dot{m}$.

The main problem with the "best" model is that the flux produced by that model is a factor of 5 times lower than required, if the true distance of IX Vel is 95 pc. (The model also underpredicts the flux within 25 Å of the Lyman limit. This portion of the spectrum is, however, fairly sensitive to the surface gravity due to blending of the Lyman series, and several lines that we have identified as belonging to the wind modify the spectrum severely.) In order to match the flux (at 1425 Å) from IX Vel at a distance of 95 pc we require an accretion rate of $\dot{m} = 3 \times 10^{17}$ g s^{-1}, if there is no extinction. That model also approximates the shape of the continuum longward of Lyman-α fairly well, but is bluer overall than the observed spectrum. The new spectral window shortward of Lyman-α opened by HUT is showing its diagnostic importance for accretion disk spectrum fitting.

The discrepancy between $\dot{m}$ estimated from colors and from fluxes is not new. For example, our earlier fitting of the continuum shape of the HUT spectrum of Z Cam indicated an accretion rate 11 times lower than suggested from the estimated luminosity (Long et al. 1991). Using stellar atmospheres, Wade (1988) found that the *IUE* color indices [$\log f_{\lambda 1460}/\log f_{\lambda 1800}$ and $\log f_{\lambda 1800}/\log f_{\lambda 2800}$] of a group of novalike variables were all too red to be reconciled with their luminosities.

We now consider this continuum shape—flux discrepancy from several points of view. Can reasonable adjustments in the model parameters allow a satisfactory fit to both shape and

© American Astronomical Society • Provided by the NASA Astrophysics Data System

1994ApJ...426..704L

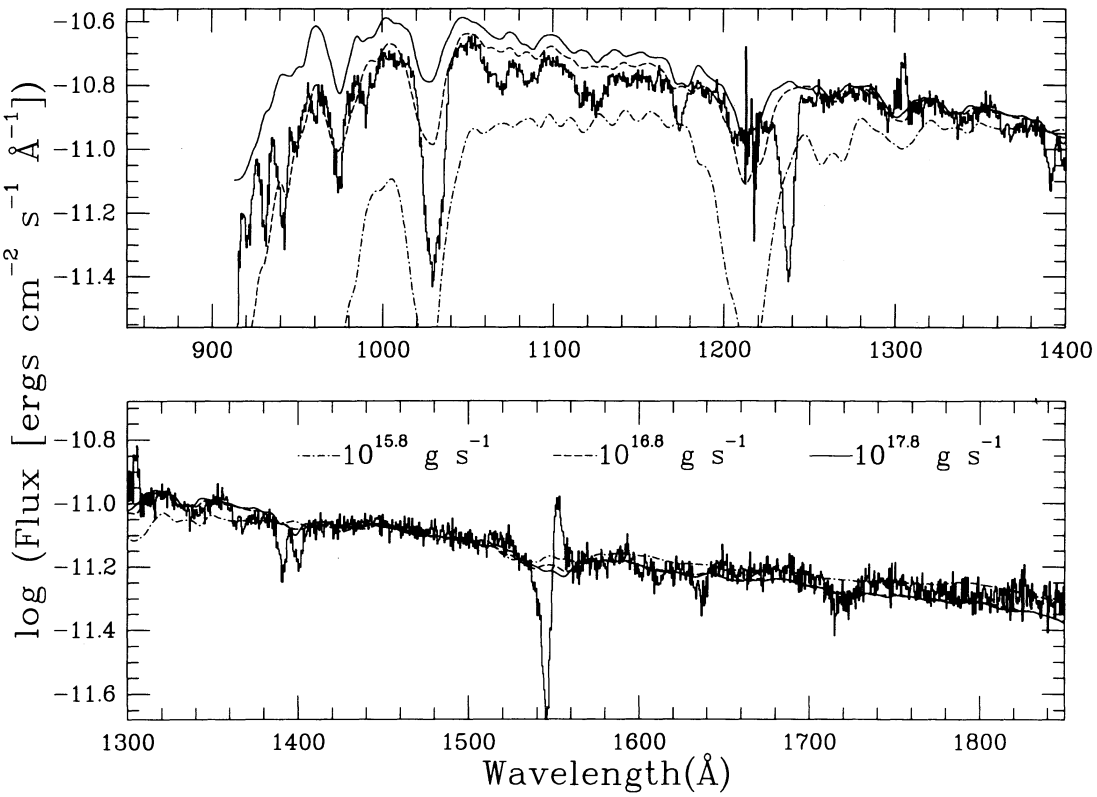

FIG. 5.—Comparison between the IX Vel spectrum and three models with accretion rates ranging from 6×10^{15} to 6×10^{17} g s^{-1}. BT had previously derived an accretion rate of 5×10^{17} g s^{-1} from a collection of data *IUE* and ground-based optical and IR spectra. In terms of the overall spectral shape, the model with 6×10^{16} g s^{-1} is best. But the flux from this model is 5 times lower than the observed flux if IX Vel is a distance of 95 pc. All of the models have been normalized to the flux observed from IX Vel at 1425 Å. To get the model flux to agree with the observed flux, IX Vel would need to be located at 11, 42, and 120 pc for $\dot{m}$ of 6×10^{15}, 6×10^{16}, and 6×10^{17} g s^{-1}, respectively.

flux level? Is the assumption of zero reddening benign? Are components of the IX Vel system other than the disk in fact negligible in the far-UV, as we have assumed so far? Or does the discrepancy between model and observation require a fundamental modification of the disk model?

1. *Adjustment of model parameters*—The $\dot{m} = 6 \times 10^{16}$ g s^{-1} model has a run of effective temperature with dimensionless radius that is characterized by $T_* = 79{,}000$ K, when the adopted values of M_{wd} and R_{wd} are used. The maximum temperature in the disk is $T_{eff}(\max) = 0.49\ T_* = 39{,}000$ K. Neglecting subtleties due to gravity and limb darkening, any disk model having the same $T_* \propto (M_{wd}\dot{m}/R_{wd}^3)^{1/4}$ will have the same continuum shape in the far-UV. Altering the size of the disk (by changing M_{wd} and hence R_{wd}, with a countervailing change in $\dot{m}$) will alter the luminosity of the disk, $L \propto R_{wd}^2$, and hence the observed flux. Altering the distance or the orbital inclination of the model will also change the flux, via $f \propto L \cos i/d^2$.

Each of the parameter values that we have adopted from BT's study has an associated error estimate. Decreasing M_{wd} by 0.11 $M_\odot$ (1 σ) increases R_{wd} by only about 10%, far less than required to account for the flux discrepancy by this means alone. (A factor of 1.6 increase in $\dot{m}$ would be required to keep $T_* = 79{,}000$ K.)

The distance estimate to IX Vel is based primarily on the flux and spectral type of the secondary star, but indirectly by means of the ellipsoidal variations detected in the infrared K band (Haug 1988). The *statistical* error of ± 12 pc given by BT includes uncertainties in the measured size of the ellipsoidal variation and in the infrared surface brightness of the secondary star, which is inferred from the radius of the star as derived from the orbital solution. The predicted size of the ellipsoidal modulation also depends on the adopted orbital inclination, so errors in cos i and d are correlated. The derived stellar radius also depends on the adopted inclination, via $R_2/a = f(q)$ and $a \sin i = P(K_1 + K_2)/2\pi$, where $f(q)$ is a function of the mass ratio, a is the semimajor axis, and K_1 and K_2 are the velocity semiamplitudes of the stars. Let the portion of the K-band flux that is ellipsoidally modulated be approximated by $\Delta F_K = S_K g(q)(\pi R_2^2/d^2) \sin i$. Here $g(q)$ is a "geometrical" form factor that accounts for the shape, limb darkening, and gravity darkening of the rotationally distorted star, for inclinations near the adopted value. S_K is the K-band surface brightness, which varies only slowly with spectral type (or radius, for main-sequence stars). Since ΔF_K is observed and $R_2 \propto 1/\sin i$, we find that $d^2 \sin i$ is an approximate observational invariant. But $F_{disk} \propto \cos i/d^2$ (neglecting limb darkening), so $F_{disk} \propto \cos i \sin i$. Taking account of these correlations among parameters, we find that altering i from the adopted 60° to 55° increases the received flux by about 8% (with no limb darkening) or 24% (with full linear limb darkening). The upshot is that altering d and i together (as required) within the estimated 1 σ errors cannot increase the flux of the $\dot{m} = 6 \times 10^{16}$ g s^{-1} model enough to agree with the HUT observa-

© American Astronomical Society • Provided by the NASA Astrophysics Data System

1994ApJ...426..704L

tions. Treating the *statistical* errors of d separately results in a possible 25% increase in the received flux, with the same conclusion as to its inadequacy.

2. *Interstellar reddening*—Introducing reddening can allow the use of a higher $\dot{m}$ with a bluer intrinsic spectrum. We fitted the IX Vel spectrum to a set of models in which the distance was fixed at 95 pc, but in which $\dot{m}$ and the reddening were allowed to vary. We used Seaton's (1979) extinction law supplemented with data from Longo et al. (1989). The best fit, which is shown in Figure 6 as the dashed line, is clearly a better fit to the data than any of the models that do not include reddening. The best fit is obtained when $E(B-V) = 0.07$ mag and $\dot{m} = 8 \times 10^{17}$ g s^{-1}, more than 10 times higher than the unreddened best-fitting model. The extinction between the Lyman limit and 1850 Å varies between 1.1 and 0.6 mag for this amount of reddening.

At very low values of the reddening the correlation between $E(B-V)$ and the 2200 Å "bump" and the correlation of $E(B-V)$ and the H I column density is somewhat uncertain. If $E(B-V) = 0.07$ and if the dust along the line of sight to IX Vel were typical interstellar dust, the extinction "bump" at 2200 Å would have an amplitude of $\sim$0.21 mag above the "baseline" extinction in the UV. Verbunt (1987) was unable to discern a bump in *IUE* spectra of IX Vel and set a rough upper limit on $E(B-V)$ of 0.04 mag (see also the illustrations in La Dous 1990). Similarly, if the dust to gas ratio along the line of sight to IX Vel were typical, the reddening corresponding to column density of H I inferred by Mauche et al. (1988) corresponds to $E(B-V) \sim 0.004$ mag, roughly 15 times smaller than required by our best fit.

The best-fit value of the extinction is quite sensitive to $\dot{m}$. Figure 6 also shows (as the solid line) a fit to the data in which the reddening has been allowed to vary but in which $\dot{m}$ has been fixed at 5×10^{17} g s^{-1}, the value of $\dot{m}$ derived by BT. In this case, the best-fit value of $E(B-V)$ is 0.03 (which does not violate Verbunt's 1987 upper limit) although the overall fit is somewhat worse than the model fit in which the value of $\dot{m}$ was unconstrained. Thus reddening may help partially resolve the difference between the accretion rate derived from the flux and the accretion rate derived from the effective color of the spectrum.

3. *Other components in the spectrum*—Our models do not include a flux contribution from the WD. Based on studies of other novalike systems which have entered low states and allowed the "bare" WD to be studied (e.g., TT Ari and MV Lyr; Sion 1991), one might expect the effective temperature of the WD in IX Vel to be 50,000–75,000 K, similar to the effective temperature of the inner disk. The additional projected radiating area involved is small, however, and the WD actually occults a portion of the inner disk, so the net increase in flux is also small. With a radius of 7×10^8 cm and an effective temperature of 50,000 (75,000) K, the WD would contribute 8% (17%) and 6% (12%) of the total flux in IX Vel at 1050 and 1400 Å, respectively. This contribution is too small to resolve directly the discrepancy between best-fitting model flux and observed flux, nor would this contribution change the model continuum slope enough to require a major compensating change in $\dot{m}$ and the modeled disk flux.

Our models have also neglected emission from a boundary layer between the accretion disk and WD. In the conventional

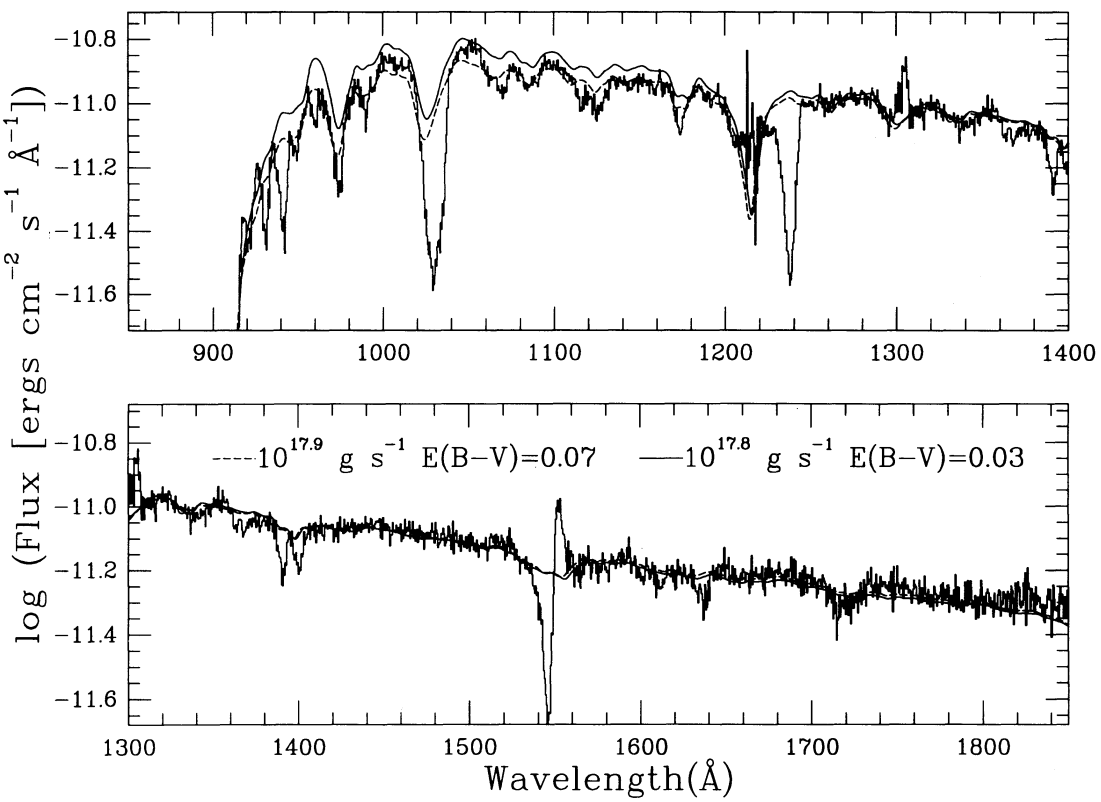

FIG. 6.—Best-fitting model, assuming a distance of 95 pc, when the absorption is allowed to vary. The best fit, which is shown as the dashed curve, has $E(B-V) = 0.07$ and $\dot{m} = 8 \times 10^{17}$ g s^{-1}. The best-fitting model in which $\dot{m}$ has been fixed at 5×10^{17} g s^{-1}, the value derived by BT, and the distance has been fixed at 95 pc is shown as the solid line. It has $E(B-V) = 0.03$.

© American Astronomical Society • Provided by the NASA Astrophysics Data System

1994ApJ...426..704L

picture of nonmagnetic CVs accreting mass at high rates, up to half the accretion energy of a CV is radiated in the boundary layer, which is optically thick (Pringle 1977; Patterson & Raymond 1985). If this picture were correct, the temperature of the boundary layer would have to be far hotter (several times 10^5 K) than the disk (because it is much smaller), and the boundary layer would be a strong extreme UV source. (See, however, § 4 for a brief discussion of recent theoretical developments.) Dwarf novae in outburst are thought to be accreting at high rates, like novalike variables, and might be expected to show similar boundary layer properties. Studies of the dwarf nova VW Hyi in superoutburst (Mauche et al. 1991; van Teeseling, Verbunt, & Heise 1993) show the EUV luminosity in that system, presumably from the boundary layer, to be only a few percent of the disk luminosity, however. Even if the contribution of the boundary layer is maximized in the far-UV region accessible to HUT, it should be only a minor contributor (of order 10% of the disk flux at 1000 Å at best; Polidan et al. 1990). It therefore is reasonable to ignore the direct effect of such a boundary layer on the overall flux of our model. The effect on the continuum shape would be to make it bluer; this exacerbates the problems posed by the disk models, which is that the models predicting the correct flux are already too blue.

To verify these qualitative arguments, we attempted models in which we added a hot ($T > 50{,}000$ K), high-gravity ($\log g = 8$) component to the spectrum of a standard disk. For all of these models, the variables were $\dot{m}$, the temperature of the boundary layer or WD, and the size of the boundary layer or WD. The best fit was obtained when the contribution of the hot component went to zero.

A bright spot, where the mass stream from the secondary star encounters the disk, produces much of the flux at optical wavelengths in some dwarf novae in quiescence, for example, U Gem (Marsh et al. 1990) or OY Car (Horne et al. 1994). The HUT observations of the eclipsing novalike variable UX UMa show a substantial pre-eclipse brightening which indicates that bright spot emission extends to much shorter wavelengths in some novalike variables. A relatively cool bright spot would require a somewhat hotter disk (and higher flux levels) than in our baseline model to produce the observed spectral shape of IX Vel. To assess whether a bright spot is important in the far UV, we carried out fits to the HUT spectrum in which the bright spot was modeled as a stellar atmosphere ($\log g = 3$). We allowed the temperature of the bright spot and the relative contribution of the bright spot and the disk to vary, but fixed the overall luminosity. The best fit was obtained when $\dot{m} = 2.3 \times 10^{17}$ g s^{-1} and $T_{\rm spot} \sim 25{,}000$ K. If this model were correct, then the bright spot would contribute about 20% of the flux at 1400 Å. But the overall fit was actually somewhat worse than the standard disk model, and thus there is no reason to invoke this as a solution to the problem.

4. *Changes in the disk model*—Recall that the nature of the far-UV fitting problem for IX Vel is that a standard accretion disk model that gives the correct UV flux predicts a continuum shape that is too blue, and a model that gives the right continuum shape in the UV uses an accretion rate that is 5 times smaller than $\dot{m}$ inferred optically by BT using the same $M_{\rm wd}$, distance, and disk inclination. In this subsection we consider ad hoc modifications of the disk structure $T_{\rm eff}(r)$ which can redden the continuum while allowing a high flux. We consider the physical meaning of such modifications in the next section. Here we merely note observationally that maps of the brightness temperature of disks in eclipsing CVs do not always show the expected $T \propto r^{-3/4}$ behavior (Rutten, van Paradijs, & Tinbergen 1992).

The ad hoc modifications of the disk are designed to remove flux preferentially from the hot inner regions of the disk. One simple possibility is to remove all flux originating inside some radius, while otherwise adhering to the standard $T(r)$ prescription; with $\dot{m}$ increased to match the required UV flux, the disk can still be redder than in the standard case. As shown by the dashed curve in Figure 7, a disk with $\dot{m}$ of 5×10^{17} g s^{-1}, the value derived by BT, in which the radiation arising inside 3.7 $R_{\rm wd}$ has been removed provides a reasonable match to both the effective color and the luminosity of the observed spectrum. A second, perhaps less extreme, modification is to replace the inner disk with $T(r) =$ constant inside some radius, again adjusting $\dot{m}$ as needed. In this case, a model with the same accretion rate, but in which the temperatures of all portions of the disk hotter than 31,000 K have been arbitrarily set to 31,000 K provides a similar fit to the data. Such "models" might crudely reproduce the effect of a loss of disk luminosity to the wind's mechanical luminosity, either total or gradually with decreasing radius. (Whether one assumes that the disk is disrupted or that the temperature is constant inside some radius, the total luminosity of the "best-fitting" model is about half that of a standard disk with $\dot{m} = 5 \times 10^{17}$ g s^{-1}.) A third possibility involves making the formal inner radius of the disk larger than the stellar radius. In the standard disk model, the luminosity of the disk $L \simeq GM\dot{m}/2R_{\rm min}$. This implies $T_* \propto L^{1/4}/R_{\rm min}^{1/2}$. As a result, for a given L, the effective temperature of the disk can be lowered by increasing the inner radius of the disk. As is shown in Figure 7, an improved fit over standard accretion disks models can be obtained while matching the observed flux at 95 pc, if we assume $R_{\rm min} \sim 2.6R_{\rm wd}$ or 1.8×10^9 cm. Thus, it is quite clear that ad hoc modifications to the inner disk can "resolve" the discrepancy between the color and the flux from IX Vel as observed with HUT.

4. DISCUSSION

We have used standard steady state accretion disk models and best estimates for the fixed parameters $M_{\rm wd}$, $R_{\rm wd}$, distance and inclination to produce synthetic spectra for comparison with the HUT spectrum of IX Vel. Since it is clear that the spectrum is modified by absorption in a strong wind that we cannot yet model, there is some uncertainty as to what a "good fit" is—should the model describe an upper envelope to the data or go among the data in the usual χ^2 sense? Nevertheless our eyes generally agree with numerical measures, and we find that our basic model with one free parameter ($\dot{m}$) can either match the overall shape of the HUT data reasonably well while underpredicting the flux, or match the flux but predict a spectral energy distribution that is slightly too blue. These conclusions do not depend on the details of the model fitting procedure, that is, on whether the data are weighted uniformly or by counting statistics, or on how the models are constructed (within the framework of nonirradiated hydrostatic LTE atmospheres). The discrepancy between $\dot{m}$ determined from color or from flux is less than an order of magnitude, which is satisfactory for some purposes. It is less than a resounding success, when IX Vel is regarded as a test case for a modeling procedure that is to be applied in more complex (i.e., nonsteady) situations.

In seeking ways to improve the fit between model and data we have considered adjustment of the fixed model parameters within their statistical uncertainties, interstellar reddening, and

© American Astronomical Society • Provided by the NASA Astrophysics Data System

1994ApJ...426..704L

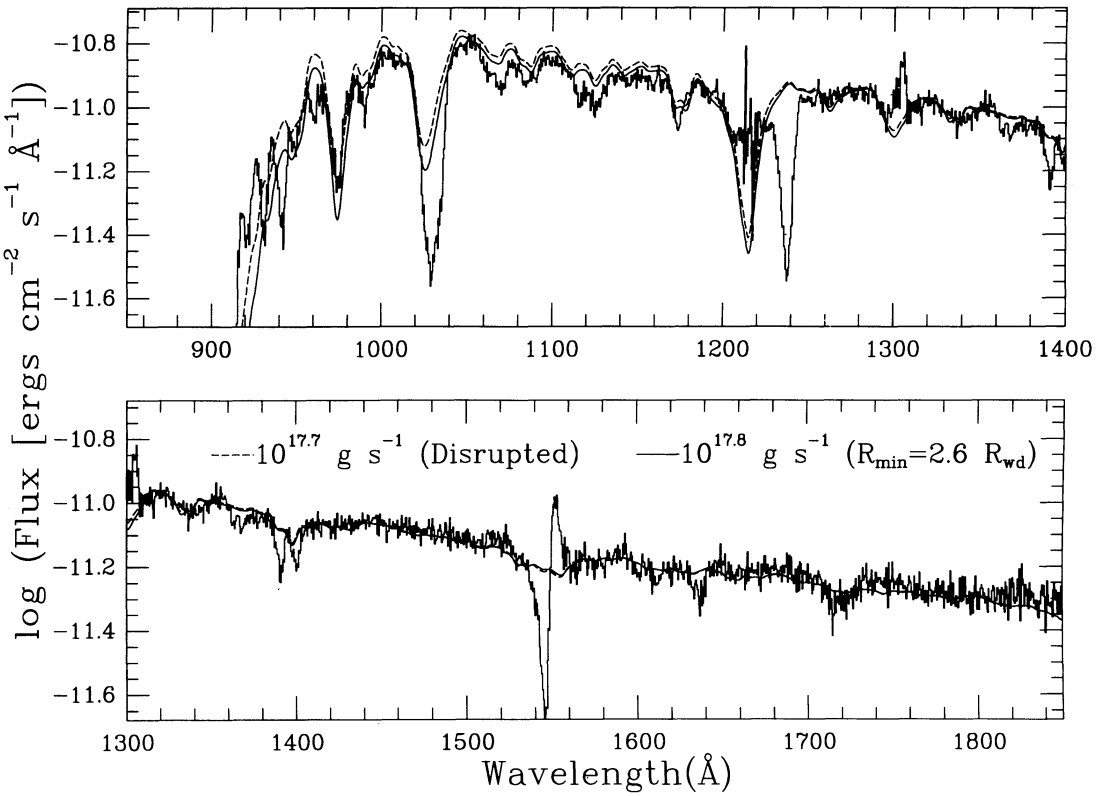

FIG. 7.—Two modified-disk models which match the flux from IX Vel assuming a distance of 95 pc. In the model shown as the dashed curve light, radiation from the hot ($T > 42{,}000$ K) portion of a standard disk with $\dot{m}$ of 5×10^{17} g s^{-1} has simply been removed. This corresponds to removing all of the light inside of 2.6×10^9 cm or $3.7R_{wd}$. In the model shown as the solid curve, the inner accretion disk radius was increased to 1.8×10^9 cm or $2.6R_{wd}$ and the accretion rate was 6×10^{17} g s^{-1}.

other components in the spectrum. Of these, only reddening appeared to improved the match between color and flux without violating some other constraint on the system. A trigonometric parallax for IX Vel should someday be available from *Hipparcos*; being confident of the distance to the source is vital for interpreting any model discrepancies. Pending such revision of basic data, and provided the basic modeling procedure is right, we are led to consider modifications of the standard disk structure. We also showed in the preceding section that flux and color matches can be improved if the usual $T_{eff}(r)$ recipe is modified in the inner disk. Is this justifiable?

The usual $T_{eff}(r)$ formula arises from solving a diffusion equation for the disk assuming time independence, transport of angular momentum by viscous (i.e., local) processes, and circular orbits obeying a Keplerian law, $\Omega \propto r^{-3/2}$, except in a small region near the surface of the accreting star (the boundary layer). All energy liberated by accretion is assumed to be radiated from the faces of the disk, which is geometrically thin. With these assumptions the diffusion equation has a simple solution with one constant of integration, determined by setting $\Omega' \equiv d\Omega/dr = 0$ in the boundary layer. (See Pringle 1981 or Frank, King, & Raine 1992 for details.) To obtain a different $T_{eff}(r)$, one or more of these assumptions must be altered. If $\Omega' = 0$ is attained at a place other than the star-disk interface, then the boundary condition is altered, and some disk orbits are no longer Keplerian. As shown recently by Popham et al. (1993), this is exactly what follows from more sophisticated calculations which solve for the radial momentum and energy flow correctly. They show that the basic effect, neglected by the canonical model, is a significant radial flow of energy generated in the "dynamical boundary layer" where Ω drops from Keplerian to the stellar rotation rate. Therefore, the "thermal boundary layer" is more extended, and consequently the $T_{eff}(r)$ law is shallower than predicted by the canonical model (though in Popham et al.'s models the effect does not extend to 3 times the inner accretion disk radius). A similar situation might also obtain if the inner disk were forced by a stellar magnetic field to corotate with the star inside a magnetic radius R_M, as presumably happens in the DQ Her stars. Alternatively, a wind could carry away some of the disk luminosity in mechanical form, altering $T_{eff}(r)$.

A stellar magnetic field with surface strength $B \sim 10^6$ G (e.g., Frank et al. 1992) would be required to dominate the flow of matter within a few stellar radii of the surface. The magnetically dominated flow onto the star would be expected to be radial, resulting in strong local heating and copious X-ray emission, which has not been reported for IX Vel. Another signature of polar accretion (if the magnetic pole is not aligned with the rotation pole of the star) would be strictly coherent pulsations in the optical waveband, reflecting the rotation of a polar hot spot into and out of view, but none were found by Williams & Hiltner (1984) or Warner et al. (1985), although the latter study found occasional oscillations in the period range 24–29 s. If these oscillations reflect orbital motion of "blobs" around the WD, then the disk must extend to within one WD radius of the surface. A weaker field, perhaps $\sim 10^5$ G, might alter the torques in the disk without redirecting the flow from

© American Astronomical Society • Provided by the NASA Astrophysics Data System

1994ApJ...426..704L

primarily azimuthal to radial (see Livio & Pringle 1992 for a discussion of weak fields in the context of dwarf nova disks).

On the other hand, a wind signature is certainly evident in the spectrum of IX Vel, as also in the spectra of Z Cam (observed with HUT; Long et al. 1991) and other novalike CVs (observed with *IUE*, e.g., Mauche et al. 1988). These other systems lead to similar difficulties in matching model disk spectra to the observations. It may be that a strong wind signature is a sign that altered disk structures should be considered.

5. CONCLUSIONS

Using the Hopkins Ultraviolet Telescope we have obtained a high-quality spectrum of the novalike variable IX Vel in the wavelength range between 830 and 1860 Å. Below Lyman-α many absorption lines are evident, most of which are blue-shifted by 3–4 Å. There is no evidence of emission below 912 Å in our spectrum. Our analysis of the spectrum in terms of accretion disk models leads to the following conclusions:

1. The strength, narrowness, and blueshifts of the high ionization state lines suggests that they must arise due to scattering in the wind from IX Vel. Many of the intermediate ionization state lines are likely to be affected by the wind as well. C III λ977, Lyman-β, Lyman-α, and Si III $\lambda\lambda$1295–1303 are likely to be the most prominent disk lines in the spectrum of IX Vel.

2. Although the absorption lines hamper our ability to compare quantitatively the continuum emission from IX Vel with accretion disk models, the spectrum (both above and below Lyman-α) is broadly consistent with that expected from a steady state disk.

3. In the standard accretion disk model for high mass-transfer CVs, optical depths at UV wavelengths are high. As a result, the disk spectra calculated using the method of Kriz & Hubeny (1986) which more correctly calculate the vertical structure of the disk are almost identical to model spectra synthesized from stellar atmospheres in the UV (at least at HUT's moderate spectral resolution).

4. If the reddening along the line of sight to IX Vel is low and if the orbital parameters and distance estimates for IX Vel are approximately correct, there is a difference in the accretion rate of IX Vel derived from the luminosity (3×10^{17} g s^{-1}) and the color (6×10^{16} g s^{-1}) in the context of the standard steady state model.

5. Better agreement within the context of the standard accretion disk model can be obtained if the reddening is higher than is suggested by the absence of a 2200 Å bump and by the very low H I column density measured by Mauche et al. (1988).

6. Improved fits to the data with no reddening can also be obtained if the structure of the accretion disk within about three WD radii is modified (so that the effective temperature is lower there than the standard model would predict). A modified disk structure might result from the effect of the wind or the magnetic field on the system.

IX Vel is a well-studied and simple system compared with most other CVs and therefore is key to the confrontation between theory and observation. The HUT spectrum provides stark evidence that present models are inadequate. Our analysis indicates that there is probably no point in improving models of vertical structure keeping the radial structure fixed by the canonical disk model. We feel that further progress will require solving simultaneously for the radial momentum and energy flow as well as for the vertical structure.

This work is supported by NASA contract NAS 5-27000 to the Johns Hopkins University and by NASA grant NAGW-3171 to the Pennsylvania State University.

REFERENCES

Beuermann, K., & Thomas, H.-C. 1990, A&A, 230, 326 (BT)
Davidsen, A. F., et al. 1992, ApJ, 392, 264
Drew, J. E. 1987, MNRAS, 224, 595
Eggen, O. J., & Niemela, V. S. 1984, AJ, 89, 389
Frank, J., King, A., & Raine, D. 1992, Accretion Power in Astrophysics (2d ed.; Cambridge: Cambridge Univ. Press)
Garrison, R. F., Schild, R. E., Hiltner, W. A., & Krzeminski, W. 1984, ApJ, 276, L13
Haug, K. 1987, Ap&SS, 130, 91
———. 1988, MNRAS, 235, 1385
Herter, T., Lacasse, M. G., Wesemael, F., & Winget, D. E. 1978, ApJS, 39, 513
Hoare, M. G., & Drew, J. E. 1993, MNRAS, 260, 647
Horne, K., Marsh, T. R., Cheng, F.-H., Hubeny, I., & Lanz, T. 1994, ApJ, in press
Hubeny, I. 1988, Comput. Phys. Comm., 52, 103
———. 1990, ApJ, 352, 632
———. 1994a, in Interacting Binary Stars, ed A. Shafter (ASP Conf. Series), in press
———. 1994b, Tlusty and Synspec: A User's Guide, in press
Kriz, S., & Hubeny, I. 1986, Bull. Astron. Inst. Czechoslovakia, 37, 129
Kurucz, R. L. 1990, Trans IAU 20B, 1968
———. 1993, in IAU Colloq. 138, Peculiar vs. Normal Phenomena in A-type and Related Stars, ed. M. M. Dworetsky, F. Castelli, & R. Faraggiana (San Francisco: ASP), 87
LaDous, C. 1990, Space Sci. Rev., 52, 203
Livio, M., & Pringle, J. E. 1992, MNRAS, 259, 23P
Long, K. S. 1993, in Cataclysmic Variables and Related Physics, ed. O. Regev & G. Shaviv, Ann. Israeli Phys. Soc., 10, 24
Long, K. S., et al. 1991, ApJ, 381, L25
Longo, R., Stalio, R., Polidan, R. S., & Rossi, L. 1989, ApJ, 339, 474
Lynden-Bell, D., & Pringle, J. E. 1974, MNRAS, 168, 603
Marsh, T. R., Horne, K., Schlegel, E. M., Honeycutt, R. K., & Kaitchuck, R. H. 1990, ApJ, 364, 637
Mauche, C. W. 1991, ApJ, 373, 624
Mauche, C. W., & Raymond, J. C. 1987, ApJ, 323, 690
Mauche, C. W., Raymond, J. C., & Córdova, F. A. 1988, ApJ, 335, 829
Mauche, C. W., Wade, R. A., Polidan, R. S., van der Woerd, H., & Paerels, F. F. S. 1991, ApJ, 372, 659
Patterson, J., & Raymond, J. C. 1985, ApJ, 292, 550
Polidan, R. S., Mauche, C. W., & Wade, R. A. 1990, ApJ, 356, 211
Popham, R., Narayan, R., Hartmann, L., & Kenyon, S. 1993, ApJ, 415, L127
Pringle, J. E. 1977, MNRAS, 178, 195
———. 1981, ARA&A, 19, 137
Rutten, R. G. M., van Paradijs, J., & Tinbergen, J. 1992, A&A, 260, 213
Seaton, M. J. 1979, MNRAS, 187, 73P
Shaviv, G., & Wehrse, R. 1986, A&A, 159, L5
———. 1991, A&A, 251, 117
Shlosman, L., & Vitello, P. 1993, ApJ, 409, 372
Sion, E. M. 1985, ApJ, 292, 601
———. 1991, AJ, 102, 295
van Teeseling, A., Verbunt, F., & Heise, J. 1993, A&A, 270, 159
Verbunt, F. 1987, A&AS, 71, 339
Vitello, P., & Shlosman, I. 1993, ApJ, 410, 815
Wade, R. A. 1984, MNRAS, 208, 381
———. 1988, ApJ, 335, 394
Wargau, W., Drechsel, H., Rahe, J., & Bruch, A. 1983, MNRAS, 204, 35P
Warner, B., O'Donoghue, D., & Allen, S. 1985, MNRAS, 212, 9P
Williams, G. A., & Hiltner, W. A. 1984, MNRAS, 211, 629

© American Astronomical Society • Provided by the NASA Astrophysics Data System